Materials LAB

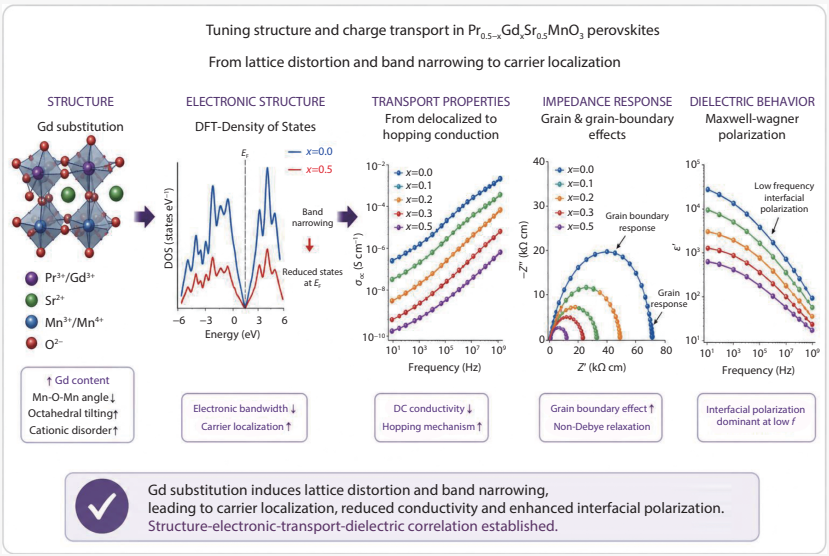
RESEARCH ARTICLE

Materials Lab 2026, 5, 260111

Multiscale transport and first-principles investigation of $Pr_{0.5-x}Gd_xSr_{0.5}MnO_3$ ($0 \leq x \leq 0.3$) perovskites: from polaronic conduction to interface-driven dielectric relaxation

A. Ben Jazia Kharrat*

In this work, we present a comprehensive investigation of the structural, electronic, and dielectric properties of Gd-substituted $Pr_{0.5-x}Gd_xSr_{0.5}MnO_3$ ($0 \leq x \leq 0.3$) perovskites using a combined experimental reinterpretation and first-principles approach. Structural distortion induced by Gd incorporation leads to significant modifications in charge transport mechanisms. Direct Current (DC) conductivity reveals thermally activated behavior governed by small polaron hopping, while Alternating Current (AC) conductivity exhibits a transition between Drude-like metallic response and Jonscher-type dispersive conduction. Impedance spectroscopy confirms dominant grain-boundary contributions and non-Debye relaxation. Density Functional Theory (DFT) calculations reveal progressive band narrowing and increased carrier localization with increasing Gd content, consistent with experimental activation energies. The correlation between electronic structure and transport properties is established, providing a predictive framework for defect-engineered manganites. The results highlight the crucial role of interfacial effects and carrier localization in governing the functional properties of complex oxide materials.



Perovskite manganites with the general formula ABO_3 have attracted considerable attention owing to their rich interplay between structural, electronic, and magnetic degrees of freedom which gives rise to a wide spectrum of functional behaviors relevant for modern electronic and energy applications[1]. Among these materials, half-doped systems such as $Pr_{0.5}Sr_{0.5}MnO_3$ occupy a central position because they exhibit a delicate balance between competing interactions, notably the double-exchange mechanism[2–6] responsible for metallic conductivity and the localization effects associated with lattice distortions and electron–phonon coupling. This competition leads to complex phase transitions and transport phenomena that are highly sensitive to external perturbations such as temperature, frequency, and chemical substitution.

Among the various manganite systems, $Pr_{0.5}Sr_{0.5}MnO_3$ represents a particularly attractive model compound because the half-doped composition is located near a delicate balance between ferromagnetic metallic and charge-localized insulating states. This electronic instability makes the material extremely sensitive to small structural modifications induced by ionic substitution. Even slight variations in the Mn–O–Mn bond geometry can significantly affect the double-exchange interaction, carrier mobility, and phase stability[7]. Consequently, $Pr_{0.5}Sr_{0.5}MnO_3$ provides an excellent platform for investigating how Gd-induced lattice distortion influences transport mechanisms, dielectric relaxation processes, and

Laboratoire de Physique des Matériaux, Faculté des Sciences de Sfax, Université de Sfax, B. P 1171, 3000 Sfax, Tunisia

* Corresponding author, E-mail: benjaziaaida@gmail.com

Received 10 May 2026; Accepted 10 July 2026; Published online 22 July 2026

© 2026 The Author(s). *Materials Lab* published by Lab Academic Press

DOI: 10.54227/mlab.20260111

electronic structure evolution across multiple length scales.

A-site substitution with rare-earth elements constitutes an effective strategy for tuning the physical properties of manganites by introducing controlled lattice distortion and cationic disorder. In this context, the incorporation of gadolinium ions, characterized by a smaller ionic radius compared to praseodymium, induces significant modifications in the crystal structure through the reduction of the average A-site ionic radius and the alteration of Mn-O-Mn bond angles. These structural changes directly influence the electronic bandwidth and the mobility of charge carriers, thereby affecting the conduction mechanisms. Previous experimental investigations, including those reported in [8,9], have demonstrated that increasing Gd content leads to a decrease in electrical conductivity and a concomitant increase in activation energy, suggesting enhanced carrier localization and a progressive transition from metallic to semiconducting behavior[10–12].

Despite these advances, a comprehensive understanding of the underlying mechanisms governing charge transport and dielectric response in Gd-substituted manganites remains incomplete, particularly in relation to the respective roles of grain interiors and grain boundaries, the frequency dependence of conductivity, and the microscopic origin of carrier localization. Moreover, most existing studies rely predominantly on experimental observations without establishing a direct link between macroscopic transport properties and the electronic structure at the atomic scale. This gap highlights the necessity of integrating advanced theoretical approaches with experimental analysis in order to achieve a deeper and more predictive understanding of these materials.

While previous investigations have reported the structural and electrical properties of $Pr_{0.5-x}Gd_xSr_{0.5}MnO_3$ compounds, a comprehensive interpretation linking lattice distortion, charge-carrier dynamics, impedance response, and dielectric relaxation mechanisms remains limited. The present work goes beyond a conventional characterization study by providing an integrated analysis of the evolution of transport phenomena across the investigated composition range. Particular attention is devoted to the role of Gd-induced structural disorder in governing carrier localization, grain-boundary effects, and frequency-dependent electrical response. This unified approach provides deeper insight into the mechanisms controlling electrical transport in Gd-substituted manganites.

In this work, we propose a multiscale investigation of $Pr_{0.5-x}Gd_xSr_{0.5}MnO_3$ compounds combining transport modeling, impedance spectroscopy, dielectric analysis, and first-principles calculations based on Density Functional Theory. This integrated approach allows us to correlate structural distortion with electronic structure evolution and to elucidate the mechanisms responsible for the observed transition from delocalized conduction to polaronic hopping regimes. Particular attention is devoted to the role of grain boundaries and interfacial polarization in shaping the dielectric response, as well as to the influence of Gd-induced disorder on the localization of electronic states.

By establishing a direct correspondence between experimental transport parameters and theoretically derived electronic properties, this study provides a unified framework for understanding defect-mediated conduction in manganites. The results not only clarify the fundamental physics governing these systems but also offer valuable insights for the design and optimization of perovskite-based materials in applications such as sensors, energy storage devices, and electronic components operating under varying frequency and temperature conditions.

Structural properties

The structural properties of Gd-substituted $Pr_{0.5}Sr_{0.5}MnO_3$ compounds play a fundamental role in determining their electronic and transport behavior, as the delicate balance between lattice geometry and electronic interactions governs the mobility of charge carriers. The substitution of Pr^{3+} by Gd^{3+} introduces a significant modification in the crystal lattice due to the smaller ionic radius of gadolinium, which leads to a progressive reduction of the average A-site ionic radius and an increase in lattice distortion. This effect is accompanied by a structural transition from a relatively symmetric tetragonal phase in the undoped compound to a distorted orthorhombic structure at higher doping levels, as experimentally observed in [8,9]. Such a transition reflects the increasing instability of the crystal lattice under chemical substitution and highlights the sensitivity of perovskite structures to ionic size mismatch.

The distortion of the lattice is primarily manifested through the modification of the Mn-O-Mn bond angle and the Mn–O bond length, both of which are critical parameters controlling the electronic bandwidth and the efficiency of the double-exchange interaction[13–14]. As the Gd content increases, the Mn-O-Mn bond angle decreases significantly, indicating enhanced tilting of the MnO_6 octahedra (see Fig. 1). This tilting reduces the orbital overlap between manganese d orbitals and oxygen p orbitals, thereby weakening the electron hopping probability across the lattice. At the same time, a slight increase in the Mn–O bond length is observed, which further contributes to the reduction of electronic bandwidth and promotes carrier localization. These structural modifications collectively lead to a narrowing of the conduction pathways and a suppression of long-range electronic coherence (as summarized in Table 1).

In addition to bond distortion, Gd substitution introduces a notable increase in cationic disorder within the A-site sublattice, which has a profound impact on the transport properties. The presence of disorder creates local potential fluctuations that act as scattering centers for charge carriers, thereby increasing the probability of localization and enhancing polaron formation. This effect becomes more pronounced at higher doping levels, where the cumulative impact of disorder and lattice distortion leads to a significant deviation from ideal perovskite symmetry. The increase in disorder is also associated with a modification of the local structural environment, resulting in heterogeneous regions that can influence both grain and grain-boundary contributions to electrical conduction.

Interestingly, despite the reduction in the average ionic radius, the unit-cell volume slightly increases with Gd substitution, a behavior that may appear counterintuitive at first

DOI: 10.54227/mlab.20260111

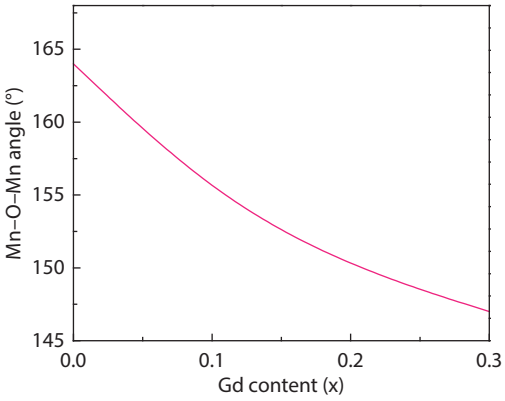


Fig. 1 Evolution of structural distortion as a function of Gd content in $Pr_{0.5-x}Gd_xSr_{0.5}MnO_3$ compounds. The progressive decrease of the Mn-O-Mn bond angle reflects the increasing tilting of MnO_6 octahedra induced by Gd substitution, leading to reduced orbital overlap and a weakening of the double-exchange interaction. This structural distortion plays a central role in the transition from delocalized to localized charge transport.

glance but can be explained by the combined effect of octahedral tilting and lattice relaxation mechanisms. The distortion of MnO_6 octahedra leads to an expansion of certain lattice parameters in order to accommodate structural strain, thereby resulting in an overall increase in unit cell volume.

This observation underscores the intricate relationship between cation substitution and lattice relaxation in perovskite oxides and underscores the importance of considering both geometric and electronic factors in understanding their physical properties.

From a broader perspective, the structural evolution induced by Gd doping directly influences the electronic transport mechanisms observed in these materials. The reduction of the Mn-O-Mn bond angle and the increase in disorder lead to a progressive transition from a regime dominated by delocalized charge carriers to one characterized by localized polaronic transport. This transition is expected to manifest in both DC and AC conductivity measurements, as well as in dielectric and impedance responses, thereby establishing a strong correlation between structure and functionality. Consequently, a detailed understanding of the structural properties provides a necessary foundation for interpreting the complex electrical behavior of Gd-substituted manganites and for developing predictive models that link microscopic distortions to macroscopic transport phenomena.

Electrical transport properties

The electrical transport properties of Gd-substituted $Pr_{0.5}Sr_{0.5}MnO_3$ compounds reveal a complex interplay between thermally activated conduction, disorder-induced localization, and frequency-dependent carrier dynamics, reflecting the progressive modification of the electronic structure with increasing Gd content. The temperature dependence of the Direct Current (DC) conductivity exhibits a characteristic semiconducting behavior over a wide range of compositions, except at higher doping levels where a transition toward metallic-like behavior emerges at elevated temperatures, as reported in [8]. This behavior indicates that charge transport in these systems is strongly governed by thermally activated mechanisms, where the mobility of carriers increases with temperature due to enhanced hopping probability.

The DC conductivity can be described by an Arrhenius-type relation for x = 0, 0.1, 0.2, and 0.3 (see Fig. 2), which reflects the activation energy required for charge carriers to overcome potential barriers within the lattice. This relation is expressed through the standard formalism of thermally activated transport:

$$\sigma_{DC} = \sigma_0 . \exp\left(-\frac{Ea}{kT}\right) \quad (1)$$

where the activation energy Ea increases systematically with Gd substitution (see Table 2), indicating a gradual strengthening of carrier localization. This trend is consistent with the structural distortion and increased disorder discussed previously, which reduce the effective overlap between electronic orbitals and hinder long-range charge transport. The relatively low activation energies indicate that charge transport is predominantly governed by a small-polaron hopping mechanism[15–16], where charge carriers are coupled with local lattice distortions and move between neighboring sites through thermally assisted processes.

In addition to DC transport, the frequency-dependent Alternating Current (AC) conductivity provides further insight into the dynamics of charge carriers and the role of disorder (as shown in Fig. 3). The AC conductivity spectra typically exhibit two distinct regimes, with a frequency-independent plateau at low frequencies corresponding to DC conduction and a dispersive region at higher frequencies associated with localized hopping processes. This behavior can be described by the universal Jonscher power law[17–20], which captures the contribution of frequency-dependent transport mechanisms:

$$\sigma_{AC}(\omega) = \sigma_{DC} + A\omega^s \quad (2)$$

where the exponent s reflects the degree of interaction between charge carriers and the surrounding lattice. The evolution of this exponent with temperature and composition provides valuable information on the underlying conduction mechanism, as values lower than unity are generally associated with long-range hopping across potential barriers, while values approaching unity indicate localized motion between neighboring sites (as listed in Table 3). In the present system, the vari-

Table 1. Structural parameters of $Pr_{0.5-x}Gd_xSr_{0.5}MnO_3$ compounds as a function of Gd content. The progressive decrease in the Mn–O–Mn bond angle and the simultaneous increase in Mn–O bond length highlight the growing lattice distortion induced by Gd substitution, while the increase in cationic disorder reflects the enhanced structural heterogeneity that directly influences charge transport mechanisms.

x	Structure	<Mn-O-Mn> (°)	<Mn-O> (Å)	Disorder
0.0	Tetragonal	164	1.949	Low
0.1	Orthorhombic	152	~1.96	Moderate
0.2	Orthorhombic	150	~1.98	High
0.3	Orthorhombic	147	~2.01	Very high

DOI: 10.54227/mlab.20260111

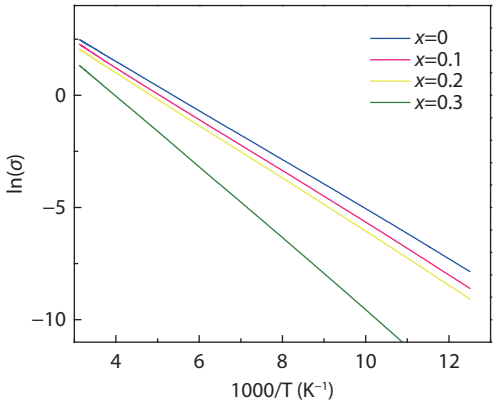


Fig. 2 Temperature dependence of DC electrical conductivity represented in Arrhenius form for different Gd concentrations. The linear behavior confirms a thermally activated conduction mechanism, while the increase in slope with Gd content indicates a rise in activation energy associated with enhanced carrier localization and disorder-induced scattering.

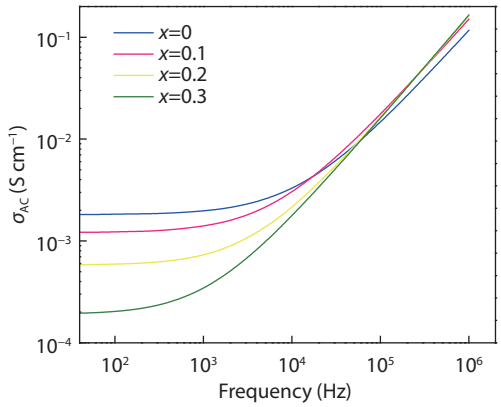


Fig. 3 Frequency dependence of AC conductivity at different temperatures and compositions. The low-frequency plateau corresponds to DC conductivity, whereas the dispersive high-frequency region follows Jonscher's power law, revealing a hopping conduction mechanism. The variation of the exponent reflects the transition between different transport regimes influenced by Gd substitution.

ation of s suggests a transition between correlated barrier hopping and non-overlapping small polaron tunneling regimes as the Gd content increases, highlighting the impact of disorder on carrier dynamics.

At higher temperatures and lower doping levels, the conductivity exhibits features characteristic of a metallic response, which can be described within the framework of the classical Drude model[21–22]. In this regime, charge carriers behave as quasi-free electrons whose motion is primarily limited by scattering processes, and the AC conductivity can be expressed as:

$$\sigma_{AC}(\omega) = \frac{\sigma_{DC}}{1+\omega^2\tau^2} \quad (3)$$

where the relaxation time τ represents the average time between scattering events. The increase of this relaxation time with temperature, observed experimentally in [8], confirms the presence of a metallic-like conduction regime in specific compositional and thermal conditions. However, this behavior is

Table 2. Activation energies derived from DC conductivity measurements for different Gd concentrations. The systematic increase in activation energy with Gd content confirms the progressive localization of charge carriers and supports the transition from a relatively delocalized conduction regime to a thermally activated hopping mechanism.

x	Ea (meV)	Conduction type
0.0	31	Semiconducting
0.1	35	Semiconducting
0.2	36	Semiconducting
0.3	67	Transition (S-M)

Table 3. Jonscher power law fitting parameters extracted from AC conductivity analysis for selected compositions. The evolution of the frequency exponent provides insight into the conduction mechanism, indicating a transition from correlated barrier hopping to localized polaron tunneling as the Gd concentration increases, in agreement with the observed increase in carrier localization.

x	Exponent s	Mechanism
0.2	<1	Correlated Barrier Hopping (CBH)
0.3	>1	Non-overlapping Small Polaron Tunneling (NSPT)

progressively suppressed with increasing Gd content, as disorder and lattice distortion promote carrier localization and reduce the effectiveness of coherent transport.

The coexistence of several transport mechanisms reflects the intrinsic heterogeneity introduced by chemical substitution and structural disorder. At low temperatures, the dominance of localized hopping indicates that charge carriers are confined within potential wells created by disorder and lattice imperfections. As the temperature increases, thermal activation enables carriers to overcome these barriers, leading to enhanced mobility and, in some cases, a transition toward metallic conduction. This duality between localized and delocalized transport regimes is a hallmark of strongly correlated oxide systems and underscores the importance of considering both structural and electronic factors in interpreting their transport behavior.

Overall, the electrical transport properties of Gd-substituted $Pr_{0.5}Sr_{0.5}MnO_3$ reveal a continuous evolution from a relatively delocalized conduction regime to a strongly localized one as the level of substitution increases. This evolution is governed by the combined effects of lattice distortion, cationic disorder, and electron–phonon interactions, which collectively determine the mobility and dynamics of charge carriers. The detailed analysis of both DC and AC conductivity thus provides a comprehensive picture of the transport mechanisms operating in these materials and establishes a direct link between structural modifications and electronic behavior.

Compared with previous studies on Pr-based manganites, the present results show consistent trends in the reduction of electrical conductivity and the increase in activation energy with increasing Gd content. Rahmouni et al. reported that Gd substitution in $Pr_{0.5}Sr_{0.5}MnO_3$-based compounds enhances carrier localization and promotes thermally activated transport, which agrees with the increase in activation energy observed in the present work. Similarly, Jemai et al. showed that structural distortion induced by rare-earth substitution weakens the Mn–O–Mn orbital overlap and favors a transition from delocalized to localized transport. The present study extends these findings by correlating the evolution of DC conductiv-

DOI: 10.54227/mlab.20260111

ity, AC conductivity, impedance response, and dielectric relaxation within a unified framework.

In comparison with other substituted manganite perovskites, the observed behavior is also consistent with the general role of A-site disorder in reducing carrier mobility and enhancing grain-boundary effects. However, the present $Pr_{0.5-x}Gd_xSr_{0.5}MnO_3$ system shows a particularly pronounced increase in activation energy at higher Gd content, indicating stronger carrier localization. This confirms that Gd substitution is an effective route for tuning the transport and dielectric properties of half-doped manganites.

Impedance spectroscopy and dielectric response

Impedance spectroscopy provides valuable insight into the charge-transport processes occurring in Gd-substituted $Pr_{0.5-x}Gd_xSr_{0.5}MnO_3$ ceramics. inside Gd-substituted $Pr_{0.5}Sr_{0.5}MnO_3$, especially in polycrystalline materials where different regions do not behave in the same way. The electrical response originates from multiple contributions associated with both grain interiors and grain boundaries, mainly originating from the grains themselves and from the grain boundaries that separate them. This complexity becomes clearly visible in the Nyquist plots reported in Fig. 4, where the impedance response deviates from an ideal semicircle and instead shows depressed arcs, a typical signature of non-Debye relaxation and distributed electrical processes.

This deviation from ideal behavior is not surprising when considering the structural disorder introduced by Gd substitution. As the lattice becomes more distorted and chemically heterogeneous, charge carriers no longer experience a single, well-defined environment, but rather a range of local potentials and barriers. As a result, their response to an applied alternating field becomes spread over a range of relaxation times. In practical terms, this means that the electrical response cannot be described by a simple capacitor or resistor, but instead requires an equivalent circuit that captures both

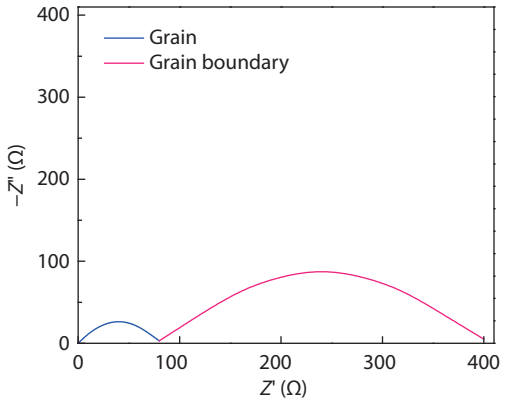


Fig. 4 Nyquist plots of complex impedance for Gd-substituted samples at selected temperatures. The presence of two depressed semicircles indicates distinct contributions from grains and grain boundaries, while their evolution with temperature highlights the thermally activated nature of charge transport. The deviation from ideal semicircular behavior reflects non-Debye relaxation and structural heterogeneity.

grain and grain-boundary contributions. The high-frequency region of the spectra is mainly associated with the intrinsic response of the grains, where carriers move more freely, while the low-frequency region reflects the influence of grain boundaries, where defects and disorder tend to trap or slow down carriers.

One particularly interesting feature that emerges with increasing Gd content is the appearance of an inductive-like contribution at low frequencies. This behavior suggests that the system does not respond instantaneously to the applied field, but instead exhibits a delayed response that may be linked to localized carriers or complex polarization effects. In other words, the material behaves not only as a resistive and capacitive system, but also shows signs of dynamic charge redistribution, which becomes more pronounced as disorder increases. At the same time, the overall resistance decreases with temperature, as indicated by the shrinking of the semicircles in the impedance plots, which is consistent with the thermally activated transport mechanisms discussed earlier.

Analysis of the frequency-dependent impedance reveals that the real part decreases significantly as the frequency increases. At low frequencies, charge carriers tend to accumulate at interfaces such as grain boundaries, leading to what is commonly referred to as space charge polarization. As the frequency increases, these carriers can no longer follow the rapidly changing electric field, and their contribution diminishes, allowing the intrinsic bulk properties to dominate. This transition from interfacial to bulk behavior provides valuable information about the mobility and dynamics of charge carriers within the material.

The imaginary part of the impedance adds another layer of understanding by revealing relaxation processes through the presence of peaks that shift toward higher frequencies as the temperature increases. This shift indicates that the relaxation dynamics are thermally activated, meaning that carriers require energy to move between localized states. The fact that these peaks are relatively broad suggests that the system does not relax through a single mechanism, but rather through a distribution of processes, again reflecting the structural and electronic disorder introduced by Gd substitution. The activation energies associated with these relaxation processes are found to be consistent with those obtained from conductivity measurements, which reinforces the overall coherence of the transport model.

The dielectric response follows a similarly intuitive behavior. At low frequencies, the dielectric permittivity reaches high values (as shown in Fig. 5) due to the accumulation of charges at interfaces, a phenomenon often described in terms of Maxwell–Wagner polarization. This effect is particularly strong in materials with significant heterogeneity, where grain boundaries act as barriers that trap charges. As the frequency increases, these charges are no longer able to respond quickly enough, and the dielectric permittivity decreases accordingly. Temperature also plays a role, as increasing thermal energy facilitates charge movement and reduces the effectiveness of interfacial polarization.

The dielectric loss, which reflects energy dissipation within the system, shows a gradual decrease with frequency and is closely linked to the hopping motion of charge carriers. In this context, energy is lost as carriers move between localized

DOI: 10.54227/mlab.20260111

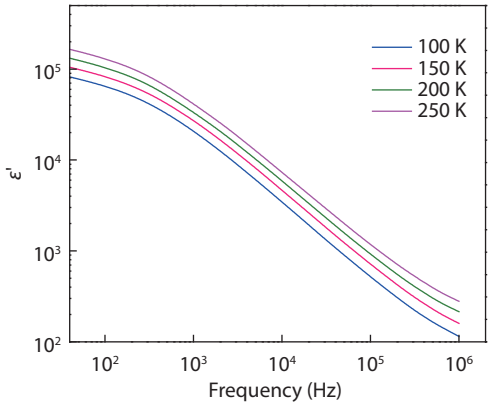


Fig. 5 Frequency dependence of dielectric permittivity for representative temperatures. The high permittivity observed at low frequencies is attributed to Maxwell–Wagner interfacial polarization, whereas the rapid decrease with increasing frequency reflects the inability of dipolar and space charge polarization mechanisms to follow the alternating electric field.

states and interact with the surrounding lattice. This process is strongly influenced by both temperature and disorder, further highlighting the role of Gd substitution in shaping the electrical behavior of the material.

Taken together, the impedance and dielectric analyses provide a more intuitive and physically meaningful picture of how charge carriers behave in Gd-substituted manganites. Rather than being governed by a single mechanism, the electrical response emerges from the combined effects of grain interiors, grain boundaries, and localized states, all of which are influenced by structural distortion and chemical disorder. This multiscale perspective is essential for understanding the transport properties of these materials and for guiding their optimization in practical applications.

First-Principles insights into electronic structure

Density Functional Theory (DFT) calculations were performed using the Vienna Ab initio Simulation Package (VASP). Exchange-correlation interactions were described within the Generalized Gradient Approximation (GGA) using the Perdew–Burke–Ernzerhof (PBE) functional. To account for the strong on-site Coulomb interactions associated with Mn 3d electrons, the GGA+U formalism[23–25] proposed by Dudarev et al. was employed. Structural optimization[26] was carried out until the residual forces on each atom were below 0.01 eV Å^{-1}. The calculated electronic density of states was subsequently used to analyze the effect of Gd substitution on carrier localization and electronic transport properties.

To gain deeper insight into the experimentally observed transport behavior, it is essential to look beyond macroscopic measurements and explore how the electronic structure evolves at the atomic scale when Gd is introduced into the lattice. In this context, first-principles calculations based on Density Functional Theory provide a valuable framework for linking structural distortion to electronic properties in a physically meaningful way. Rather than being an isolated theoretical addition, this approach allows us to interpret the experimental trends in conductivity and dielectric response from a microscopic perspective.

When considering the undoped compound, the electronic structure is characterized by a relatively broad conduction band arising mainly from the overlap between Mn 3d and O 2p orbitals. This overlap facilitates electron hopping through the well-known double-exchange mechanism[27–29], which explains the relatively higher conductivity observed at low Gd content. However, as Gd is progressively introduced into the system, the situation changes significantly. The smaller ionic radius of Gd induces lattice distortion, particularly through the reduction of the Mn–O–Mn bond angle, which directly affects the orbital overlap responsible for charge transport. As a result, the electronic bandwidth decreases and the conduction pathways become less efficient.

This evolution is clearly reflected in the calculated density of states (see Fig. 6), where a gradual narrowing of the electronic bands is observed with increasing Gd concentration. This reduction in the density of states near the Fermi level lowers the probability of carrier delocalization and suppresses electrical conduction, reducing the probability for charge carriers to move freely across the lattice. At higher doping levels, the electronic structure begins to show features consistent with a partial opening of a gap or, at least, a pronounced depletion of the density of states near the Fermi level, indicating strong carrier localization. This behavior is fully consistent with the experimental observation of increased activation energy and reduced conductivity, indicating that carriers require more energy to participate in conduction. This effect is particularly pronounced for x = 0.3, where the density of states near the Fermi level is significantly suppressed.

Another important aspect revealed by the theoretical analysis is the tendency toward charge localization. As structural disorder increases, the electronic states become more spatially confined, particularly in the vicinity of Gd ions and distorted octahedral regions. This localization favors the formation of small polarons, where charge carriers are coupled to local lattice distortions and move through thermally activated hopping rather than coherent band transport. This pic-

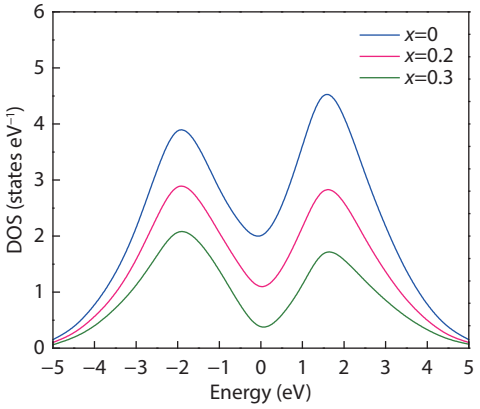


Fig. 6 Calculated density of states illustrating the effect of Gd substitution on the electronic structure. The progressive narrowing of the electronic bands and the reduction of states near the Fermi level indicate increased carrier localization, in agreement with the experimentally observed increase in activation energy and decrease in electrical conductivity.

DOI: 10.54227/mlab.20260111

ture aligns remarkably well with the transport analysis discussed earlier, where the conduction mechanism was identified as being dominated by polaronic hopping at higher doping levels.

From a quantitative point of view, the energy barriers associated with carrier motion extracted from the theoretical framework are of the same order of magnitude as the activation energies obtained experimentally. This agreement is particularly important, as it confirms that the increase in activation energy with Gd content is not simply a phenomenological observation but has a clear microscopic origin related to band narrowing and enhanced localization. In other words, the DFT results provide a solid physical justification for the transport models used to describe the conductivity behavior.

In addition to bulk electronic effects, the theoretical analysis also helps to rationalize the strong influence of grain boundaries observed in impedance measurements. The presence of localized states and reduced carrier mobility implies that any additional structural discontinuity, such as a grain boundary, will further impede charge transport and enhance interfacial polarization. This explains why grain-boundary resistance becomes dominant at certain temperatures and frequencies, and why the dielectric response is strongly influenced by Maxwell-Wagner-type effects.

Overall, the integration of first-principles calculations into the analysis provides a coherent and intuitive understanding of how Gd substitution modifies the electronic landscape of $Pr_{0.5}Sr_{0.5}MnO_3$. Rather than treating structural distortion, transport behavior, and dielectric response as separate phenomena, this approach reveals that they are all interconnected through the evolution of the electronic structure. The progressive transition from a relatively delocalized system to a strongly localized one emerges naturally from this perspective, offering a unified explanation for the experimental observations.

This combined experimental and theoretical framework not only strengthens the scientific robustness of the present study but also enhances its predictive capability. By understanding how structural parameters influence electronic properties at the microscopic level, it becomes possible to design and optimize perovskite materials with tailored transport and dielectric characteristics for specific applications.

Conclusion

The present study provides a coherent and physically grounded understanding of the electrical behavior of Gd-substituted $Pr_{0.5}Sr_{0.5}MnO_3$ by combining transport analysis, impedance spectroscopy, dielectric investigation, and first-principles insights into the electronic structure. Rather than treating these aspects separately, the results reveal a continuous and consistent evolution of the material's properties driven by structural distortion and disorder introduced through Gd substitution.

As the Gd content increases, the progressive reduction of the Mn–O–Mn bond angle and the enhancement of cationic disorder lead to a gradual transformation of the conduction mechanism. The system evolves from a regime where charge carriers can move relatively freely toward a strongly localized regime dominated by thermally activated hopping. This transition is clearly reflected in the increase of activation energy, the modification of AC transport behavior, and the emergence of non-Debye relaxation phenomena. At the same time, impedance spectroscopy highlights the growing importance of grain boundaries, which act as barriers to charge transport and play a key role in shaping the overall electrical response.

A key outcome of this study is the excellent agreement between experimental observations and theoretical interpretation. The first-principles analysis shows that Gd substitution induces a narrowing of the electronic bands and a reduction of the density of states near the Fermi level, which directly explains the observed decrease in conductivity and the tendency toward charge localization. This consistency between macroscopic measurements and microscopic interpretation provides a solid and unified picture of the mechanisms governing transport in these materials. Beyond the specific system studied here, the results underline a more general principle that is highly relevant for functional oxides, namely that subtle structural modifications can profoundly alter electronic behavior through their impact on orbital overlap and carrier mobility. In this sense, the present work does not only describe a particular manganite system but also contributes to a broader understanding of how disorder, interfaces, and electronic structure interact in complex materials. By bridging the gap between experimental characterization and theoretical modeling, this study opens the way toward a more rational design of perovskite-based materials[30] with tailored electrical and dielectric properties. Such a multiscale approach provides valuable guidelines for the rational design of next-generation oxide-based electronic devices where performance depends critically on controlling charge transport at multiple scales, from the atomic level to the microstructure.

The originality of this work lies in the establishment of direct correlations between Gd-induced structural distortion, carrier localization, impedance characteristics, and dielectric relaxation behavior. By combining complementary electrical characterization techniques within a unified framework, the study provides a deeper understanding of the mechanisms governing charge transport in $Pr_{0.5-x}Gd_xSr_{0.5}MnO_3$ compounds.

This work establishes a direct structure–transport–electronic correlation that can serve as a predictive guideline for the design of functional perovskite oxides.

■ ACKNOWLEDGEMENTS

This work has been supported by the Tunisian Ministry of Higher Education and Scientific Research.

■ CONFLICT OF INTEREST

The author declares no competing interests.

■ ETHICAL APPROVAL

Not applicable (theoretical study).

■ DATA AVAILABILITY

All data are included within this article.

DOI: 10.54227/mlab.20260111

FUNDING' DECLARATION STATEMENT

Not applicable.

AUTHOR CONTRIBUTIONS

Aida Ben Jazia Kharrat: Investigation, writing – review & editing.

REFERENCES

1. N. Q. Minh, *J. Am. Ceram. Soc.*, 1993, 76, 563–588
2. Z. C. Xia, S. L. Yuan,W. Feng, L.J. Zhang, G.H. Zhang, J. Tang, L. Liu, D.W. Liu, Q.H. Zheng, L. Chen, Z.H. Fang, S. Liu, C.Q. Tang, *Solid State Commun.*, 2003, 127, 567–572
3. N. Khare, D. P. Singh, A. K. Gupta, *J. Phys. Chem. Solids*, 2004, 65, 867–870
4. W. Boujelben, M. Ellouze, A. Cheikh-Rouhou, J. Pierre, J.C. Joubert, *J. Solid State Chem.*, 2002, 165, 375–380
5. A. K. Pramanik, A. Banerjee, *J. Phys. Condens. Matter*, 2008, 20, 275207
6. L. Chen, Y. Ma, *J. Magn. Magn. Mater.*, 2012, 324, 1189–1192
7. M. Bourouina, A. Krichene, *J. Alloys Compd.*, 2016, 680, 67–72
8. R. Jemai, H. Rahmouni, *J. Alloys Compd.*, 2017, 693, 631–641
9. H. Rahmouni, B. Cherif, K. Khirouni, *J. Alloys Compd.*, 2014, 591, 259–262.
10. J. Shanker, R. Vijaya Kumar, *J. Alloys Compd.*, 2018, 732, 314–327
11. S. Das, S. Sutradhar, *J. Alloys Compd.*, 2017, 726, 11–21
12. A. Ben Jazia Kharrat, M. Bourouina,N. Moutia, K. Khirouni, W. Boujelben, *J. Alloys Compd.*, 2018, 741, 723–733
13. C. Zener, *Phys. Rev.*, 1951, 82, 403–405
14. P. W. Anderson, H. Hasegawa, *Phys. Rev.*, 1955, 100, 675–681
15. N. F. Mott, Metal–Insulator Transitions, Taylor & Francis, London, 1990.
16. D. Emin, *Phys. Rev. B*, 1993, 48, 13691–13702
17. A. K. Jonscher, *Nature*, 1977, 267, 673–679
18. K. Funke, *Prog. Solid State Chem.*, 1993, 22, 111–195
19. J. C. Giuntini, *J. Non-Cryst. Solids*, 2002, 305, 65–70
20. A. Ghosh, *J. Appl. Phys.*, 1997, 81, 1270–1275
21. C. Kittel, Introduction to Solid State Physics, Wiley, 8th ed. ,2005.
22. N. W. Ashcroft, N. D. Mermin, Solid State Physics, Holt, Rinehart & Winston ,1976.
23. J. P. Perdew, K. Burke, M. Ernzerhof, *Phys. Rev. Lett.*, 1996, 77, 3865–3868
24. G. Kresse, J. Furthmüller, *Phys. Rev. B*, 1996, 54, 11169–11186
25. S. L. Dudarev, G. A. Botton, *Phys. Rev. B*, 1998, 57, 1505–1509
26. H. Fjellvåg, Egil Gulbrandsen, Siv Aasland, Arne Olsen, Bjørn C. Hauback, *J. Solid State Chem.*, 1996, 124, 190–194
27. E. Dagotto, Nanoscale phase separation in manganites, Springer Series ,2003.
28. Y. Tokura, *Rep. Prog. Phys.*, 2006, 69, 797–851
29. J. B. Goodenough, *Phys. Rev.*, 1955, 100, 564–573
30. A. R. West, Solid State Chemistry and Its Applications, Wiley, 2014.

©2026 The Authors. *Materials Lab* is published by Lab Academic Press. This is an open access article under the terms of the Creative Commons Attribution License, which permits use, distribution and reproduction in any medium, provided the original work is properly cited.